MRD-CI Stationary Points, Dissociation Energies, and Conical-Intersection Potentials of the Four Lowest Doublet States of NH_2

Raffaella Brandi, Erminia Leonardi, and Carlo Petrongolo*

Dipartimento di Chimica, Università di Siena, Pian dei Mantellini 44, I-53100 Siena, Italy

Received: January 31, 1997; In Final Form: April 22, 1997[⊗]

The MRD-CI equilibrium structures, transition energies, barriers to linearity, and dissociation energies of the $\tilde{X}^2B_1$, $\tilde{A}^2A_1$, and $\tilde{B}^2B_2$ electronic states of NH_2 have been calculated with large AO and natural MO bases. We have also investigated the two-dimensional potentials for the C_{2v} $\tilde{A}^2A_1/\tilde{B}^2B_2$ and $C_{\infty v}$ $1^2\Pi/1^2\Sigma^-$ conical intersections. The theoretical energies, mainly the barriers to linearity, are in good agreement with the experimental values, and the $\tilde{B}^2B_2$ state is bound with respect to its dissociation limits. The $\tilde{A}^2A_1/\tilde{B}^2B_2$ and $1^2\Pi/1^2\Sigma^-$ states intersect at energies larger than 38 000 cm^{-1} and at the beginning of the corresponding dissociation channels N + H_2 and NH + H, thus affecting the NH_2 photodissociations.

1. Introduction

Since the first works of Herzberg and Ramsay[1] and of Dressler and Ramsay[2] on the $\tilde{A}^2A_1 \leftarrow \tilde{X}^2B_1$ spectrum of NH_2, many authors investigated several structural and dynamical properties of this radical. For example, Bell and Shaefer[3] (BS) have predicted a third electronic state, $\tilde{B}^2B_2$, with a very small bond angle, and Peyerimhoff and Buenker[4] (PB), in their study on several valence and Rydberg species, have shown that $\tilde{B}^2B_2$ correlates with $1^2\Sigma_u^+$ at $D_{\infty h}$ and intersects conically the $\tilde{A}^2A_1$ state. Vetter *et al.*[5] (VZKDP) have then extended the PB work by computing vertical excitation energies and two-dimensional (2D) potentials of several states at the $\tilde{X}^2B_1$ experimental bond angle. The $1^2\Pi_u$ Renner−Teller $\tilde{A}^2A_1 \leftarrow \tilde{X}^2B_1$ rotoelectronic spectrum has been fully investigated by Jungen *et al.*[6] (JHM), by Buenker *et al.*[7] (BPPM), and by Gabriel *et al.*[8] (GCRCH), and finally Saxon *et al.*[9] (SLL), Biehl *et al.*,[10] and VZKPD have studied some photodissociations.

The first two electronic states, $\tilde{X}^2B_1$ and $\tilde{A}^2A_1$, are now well-known. However, the third, $\tilde{B}^2B_2$, state is not so well characterized: it has not been observed up to now, the older one-dimensional studies on its potential[3,4,11] were carried out with rather small basis sets for the present standard, and the recent 2D work[5] was not interested in the $\tilde{A}^2A_1/\tilde{B}^2B_2$ conical intersection. Moreover, nothing is known on the $1^2\Pi/1^2\Sigma^-$ conical intersection, which has been predicted only on symmetry grounds[12] and can be important for the photodissociation of NH_2 to NH + H.

We therefore report in this paper the results of CI calculations of the optimized equilibrium structures, barriers to linearity, and dissociation energies to NH + H and N + H_2 of the $\tilde{X}^2B_1$, $\tilde{A}^2A_1$, and $\tilde{B}^2B_2$ states, by employing large AO and natural MO bases. We have also calculated the C_{2v} and $C_{\infty v}$ 2D potentials for the conical intersections $\tilde{A}^2A_1/\tilde{B}^2B_2$ and $1^2\Pi/1^2\Sigma^-$, respectively.

The present work is complementary to the recent one by VZKDP,[5] who have investigated the NH_2 electronic vertical spectrum of several doublet states and the 2D potential surfaces of the eight lowest-lying doublets with a constant bond angle value. VZKDP have used a smaller AO basis than ours, because they were mainly interested in obtaining 2D potentials for photodissociation studies. On the other hand, the aim of our work is to calculate accurate structural data of NH_2 and to point out that two low-lying conical intersections should be taken into account in the photodissociation dynamics of NH_2.

2. Method

We have employed the well-known Buenker−Peyerimhoff multireference singles and doubles configuration interaction method (MRD-CI), with configuration selection, energy extrapolation, and full-CI estimate.[13,14]

Our AO basis comprises 122 contracted Gaussian functions: the well-tempered nitrogen[15] (14s9p) and hydrogen[16] (9s) primitive valence sets have been contracted to [6s5p] and to [6s], respectively, with the Raffenetti technique[17] and have been augmented by (3d2f) and (3d1p) polarization functions,[18] respectively, by nitrogen Rydberg AOs[19] (2s1p) and finally by (2s2p) bond functions (BFs).[7]

It has been shown that balanced basis sets which are equally good in both atomic and molecular regions should contain both nuclear- and bond-centered polarization functions.[20] The BFs polarize both bonded atoms, introduce new virtual MOs which are important at the CI level, and in most cases converge the CI energy faster than conventional polarization AOs. They therefore improve both dissociation energies and potential curves, spectroscopic constants, and vibrational levels. The effect of the BFs is therefore genuine and not due to a presumed increased basis set superposition error,[20] which is minimized in this work by a large nuclear-centered AO basis and by calculating the dissociation limits at large but finite fragment distances.

The MO basis of each electronic state has been obtained from its SCF calculations and has been transformed to a natural-orbital (NO) representation which diagonalizes a small-CI first-order density matrix. Seven electrons have been correlated among the 120 NOs, by keeping doubly occupied the nitrogen 1s and by omitting its highly excited counterpart.

Table 1 reports the technical details of the final CI calculations, both for the bound molecule and for the dissociation products: the configurations with $C^2 \geq 0.001$ define the reference set and the selection threshold is equal to 5 μhartrees. The dissociation limits NH + H or N + H_2 have been computed at the N−H or N−H_2 center-of-mass distances equal to 20 bohrs, respectively.

Our reference and selected spaces are smaller than VZKDP[5] ones because (1) the present NO bases optimize the MO spaces and therefore the CI convergence of each state; (2) VZKDP

* Corresponding author. E-mail: petro@carlo.icqem.pi.cnr.it.
[⊗] Abstract published in *Advance ACS Abstracts,* July 1, 1997.

S1089-5639(97)00390-3 CCC: $14.00

TABLE 1: Details of the MRD-CI Calculations at the Minimum Energy Points and at the Dissociations[a]

state	R	G	S	$\sum_r C_r^2$ [b]
$NH_2(\tilde{X}^2B_1, 1b_2^2 3a_1^2 1b_1)$	9	1 773 360	6007	0.960
$\tilde{A}^2A_1, 1b_2^2 3a_1 1b_1^2$	11	2 071 162	5935	0.964
$\tilde{B}^2B_2, 1b_2 3a_1^2 1b_1^2$	11	1 964 949	5999	0.961
$1^2\Pi_u, 1\sigma_u^2 1\pi_u^3$	13	1 443 038	5016	0.966
$1^2\Sigma_u^+, 1\sigma_u 1\pi_u^4$	14	1 518 307	4785	0.964
$1^2\Sigma^-, 3\sigma^2 1\pi^2 4\sigma$[c]	13	2 423 084	5557	0.965
$NH(\tilde{X}^3\Sigma^-) + H(\tilde{X}^2S_g)$	5	1 435 559	5994	0.962
$\tilde{a}^1\Delta$	15	2 668 046	5727	0.969
$\tilde{b}^1\Sigma^+$	14	2 736 769	5785	0.963
$NH(\tilde{a}^2D_u) + H_2(\tilde{X}^1\Sigma_g^+)$	21	2 678 139	4307	0.976

[a] R, G, and S are the numbers of reference, generated, and selected configurations, respectively. [b] Contribution of the reference configurations. [c] Rydberg 3s state at $D_{\infty h}$; valence state at NH + H dissociation.

TABLE 2: Equilibrium Structures, Transition Energies, and Barriers to Linearity of $\tilde{X}^2B_1$, $\tilde{A}^2A_1$, and $\tilde{B}^2B_2$[a]

state	ref	R_e	θ_e	T_e	T_v	B_l
$\tilde{X}^2B_1$	BS[3]	1.944	103.1			12 804
	BPPM[7]	1.933	102.9			12 330
	this work	1.935	105.1			12 028 ± 79[b]
	JHM[6]	1.954	102.4			12 024
	GCRCH[8]	1.938	103.7			11 914
	expt[21]	1.935	103.4			
$\tilde{A}^2A_1$	BS[3]	1.889	143.4	11 830		974
	BPPM[7]	1.871	143.0	113 50		980
	this work	1.905	148.0	11 225	16 364	803 ± 79[b]
	JHM[6]	1.903	144.2			730
	GCRCH[8]	1.882	145.9			863
	expt[c]	1.897	144.0	11 036	167 26	
$\tilde{B}^2B_2$	BS[3]	2.196	47.5	38 640		
	PB[4]	2.195	50.0	37 101	53 547	46 941
	this work	2.105	52.0	36 304	53 417	44 934 ± 77[b]

[a] R_e in bohr, θ_e in degrees, and energies in cm^{-1}. [b] Optimum R = 1.920 bohr at linearity. [c] R_e and θ_e from ref 21; T_e estimated from the experimental T_0 and from the theoretical ω_i;[8] T_v is the energy of the absorption intensity maximum.[22]

have employed $^4B_1$ SCF MOs for all the states because they were interested in several species of the same symmetry and in larger portions of 2D potentials, thus needing larger reference and selected spaces.

3. $\tilde{X}^2B_1$, $\tilde{A}^2A_1$, and $\tilde{B}^2B_2$ States

Table 2 reports the present equilibrium bond lengths R_e, bond angles θ_e, transition energies T_e, vertical energies T_v, and barriers to linearity B_l which are compared with some previous results: the theoretical ones of BS,[3] PB,[4] and BPPM;[7] the findings of JHM[6] and GCRCH[8], who have fitted some observed $\tilde{A}^2A_1-\tilde{X}^2B_1$ rovibronic levels by employing one-dimensional model and three-dimensional exact Hamiltonians, respectively; and the experimental values of Herzberg[21] and of Halpern *et al.*[22] Because the full-CI limit is perturbatively estimated, the energies at linearity of the $\tilde{X}^2B_1$, $\tilde{A}^2A_1$, and $1^2\Pi_u$ states and of the $\tilde{B}^2B_2$ and $1^2\Sigma_u^+$ ones are slightly different; we thus report in Table 2 the average values and the standard deviations of the barriers to linearity. The SCF energy and full-CI estimate of the $\tilde{X}^2B_1$ state at the calculated equilibrium structure are equal to −55.587 006 and −55.840 087 hartrees, respectively.

The present $\tilde{X}^2B_1$ and $\tilde{A}^2A_1$ *ab-initio* results reproduce accurately those of JHM[6] and GCRCH[8], whose potentials have been refined with respect to some observed energy levels. Our R_e values are within 0.02 bohr of the fitted results, and the θ_e data are 1.4−3.8° larger than those of JHM and GCRCH and closer to the more accurate latter fitting. The $\tilde{X}^2B_1$ barrier to linearity is equal to 12028 ± 79 cm^{-1}, in very good but accidental agreement with the JHM value; it is however just 114 cm^{-1} greater than the GCRCH barrier, thus improving remarkably the previous BS[3] and BPPM[7] theoretical data. We obtain similar accurate results for the $\tilde{A}^2A_1$ energies, because the differences between the present T_e, T_v, and B_l values and the experimental or GCRCH ones are equal to 189, −362, and −60 cm^{-1}, respectively. Although this finding shows that our $\tilde{A}^2A_1$ potential seems slightly too flat, the comparison of the vertical energy T_v is uncertain, because the experimental value corresponds to the intensity maximum of the absorption spectrum.[22] Our $\tilde{A}^2A_1$ most interesting result concerns the barrier to linearity of 803 ± 79 cm^{-1}: its lower and upper limits are indeed very close to the JHM and GCRCH values, respectively.

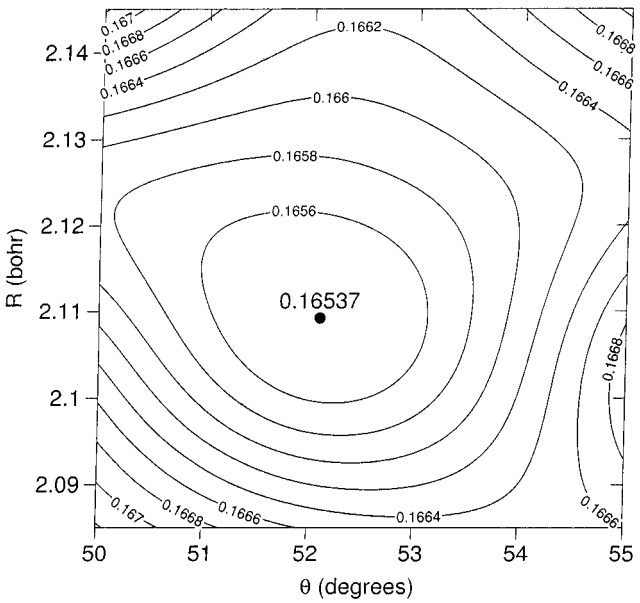

Figure 1. $\tilde{B}^2B_2$ equilibrium structure. Contour plot of the C_{2v} potential. Energy in hartree with respect to the $\tilde{X}^2B_1$ minimum.

The equilibrium structure of the third $\tilde{B}^2B_2$ state has been previously calculated by BS[3] and PB[4] with smaller AO and CI expansions. Our results confirm the large-distance and small-angle structure of this state, whose C_{2v} potential near the minimum is given in Figure 1. This surface is very flat, and its equilibrium values show that the $\tilde{B}^2B_2$ state is more stable than that predicted by BS and PB.

From the correlations between the NH_2 states and the NH + H or N + H_2 dissociation limits,[5] we have calculated the state-to-state dissociation energies D_e of the $\tilde{X}^2B_1$, $\tilde{A}^2A_1$, and $\tilde{B}^2B_2$ states of NH_2. Table 3 compares our results with previous theoretical and experimental values, where the latter are obtained from D_0,[23] from the zero-point energies,[8,24] and from the N term values.[25]

Our $\tilde{X}^2B_1$ dissociation energies to NH + H and N + H_2 are in good agreement with the experimental values, by representing more than 98% of the latter ones. This result improves remarkably the previous theoretical data of SLL[9] and VZKDP,[5] and it is due to the present larger AO basis, mainly to the bond functions, because the geometry optimization of $NH_2(\tilde{X})$ and $NH(\tilde{X})$ increases D_e by 231 cm^{-1} only. Also the theoretical $\tilde{A}^2A_1$ D_e values are close to the experiment. However, the overstimation of the NH + H dissociation limit is due to a partial cancellation of our errors for D_e of $NH_2(\tilde{X})$ and for T_e of $NH_2(\tilde{A})$ and $NH(\tilde{a})$; moreover, the larger error for N + H_2 corresponds to the greater weight of the reference configurations of this dissociation limit (see Table 1).

TABLE 3: State-to-State Dissociation Energies (cm^{-1}) of $\tilde{X}^2B_1$, $\tilde{A}^2A_1$, and $\tilde{B}^2B_2$

		NH+ H($\tilde{X}^2S_g$)		
NH_2	ref	NH	D_e	N($\tilde{a}^2D_u$) + H_2($\tilde{X}^1\Sigma_g^+$) D_e
$\tilde{X}^2B_1$	SLL[9]	$\tilde{X}^3\Sigma^-$	31 133	
	VZKDP[5]		32 101	
	this work		33 752	43 860
	expt		34 326[a]	44 504[b]
$\tilde{A}^2A_1$	this work	$\tilde{a}^1\Delta$	36 141	32 635
	expt		35 856[c]	33 468[d]
$\tilde{B}^2B_2$	BS[3]			6900
	PB[4]			6763[e]
	this work	$\tilde{b}^1\Sigma^+$	19 143	7556

[a] From the experimental[23] D_0 and from NH_2 theoretical[8] and NH experimental[24] ω_i and x_{ij}. [b] From the D_0 values[23,24] of $NH_2(\tilde{X})$, NH($\tilde{X}$), and $H_2(\tilde{X})$ and from the N($\tilde{a}$) term value,[25] corrected for the zero-point energies.[8,24] [c] From D_e of $NH_2(\tilde{X}) \rightarrow NH(\tilde{X}) + H(\tilde{X})$, $T_e(NH_2, \tilde{A})$ of Table 2, and T_e(NH, $\tilde{a}$).[24] [d] From D_e of $NH_2(\tilde{X}) \rightarrow N(\tilde{a}) + H_2(\tilde{X})$ and $T_e(NH_2, \tilde{A})$ of Table 2. [e] From the calculated energy of N($\tilde{X}$) + $H_2(\tilde{X})$ and the experimental term value of N($\tilde{a}$).[25]

TABLE 4: Equilibrium Bond Lengths and Energies of the NH States[a]

state	R_e	T_e
$\tilde{X}^3\Sigma^-$	1.978 (1.958)	
$\tilde{a}^1\Delta$	1.974 (1.954)	13 614 (12 566)
$\tilde{b}^1\Sigma^+$	1.939 (1.958)	21 965 (21 202)

[a] Distance in bohr, energies in cm^{-1}, and experiment[24] in parentheses.

The $\tilde{B}^2B_2$ state is bound by 19 413 or 7556 cm^{-1} with respect to NH + H or N + H_2, respectively, and it can thus support several rovibrational bound states and resonances because its potential surface is very flat near the minimum. The dissociation energy to N + H_2 is larger than that estimated by BS[3] or PB,[4] in agreement with the respective equilibrium structures given in Table 2. However, a nearly vertical dipolar transition from the ground state in C_s symmetry gives a weak photodissociation[9] to NH + H and a stronger one to N + H_2, because the $\tilde{B}^2B_2$ T_v energy is 2030 cm^{-1} below and 9557 cm^{-1} above the two dissociation limits, respectively.

Finally, Table 4 compares the theoretical and experimental equilibrium structures of the first three electronic states of NH, which belong to the corresponding NH + H($\tilde{X}$) dissociation limits of NH_2. Our transition energies T_e of the NH states $\tilde{a}^1\Delta$ and $\tilde{b}^1\Sigma^+$ are overestimated by 1048 and 763 cm^{-1} with respect to the experimental values,[24] which seem difficult to reproduce theoretically. These errors are indeed larger than those we have obtained for NH_2, and only Staemmler and Jacquet[26] have calculated a better $T_e(\tilde{a}^1\Delta)$ probably because their AO basis is more suitable for NH than ours.

4. $\tilde{A}^2A_1/\tilde{B}^2B_2$ and $1^2\Pi/1^2\Sigma^-$ Conical Intersections

The conical intersection between the $\tilde{A}^2A_1$ and $\tilde{B}^2B_2$ states has been previously investigated with a smaller AO basis, by calculating the nonadiabatic vibronic couplings and a diabatic representation along some one-dimensional cross sections.[11] For example, it has been found that these states intersect at R = 1.935 bohr (the experimental ground state value) and $\theta \approx 64.5°$, at about 40 150 cm^{-1} above the $\tilde{X}^2B_1$ minimum value. Nevertheless, the $\tilde{B}^2B_2$ bond length is somewhat larger than that of the ground state (see Table 2), and we have therefore investigated the C_{2v} potentials of these two states with the present larger AO basis.

Figure 2 shows the $1^2A'$ and $2^2A'$ adiabatic potentials in the region of their conical intersection; the dashed line represents the intersection locus; the C_{2v} symmetry of the lower $1^2A'$ is

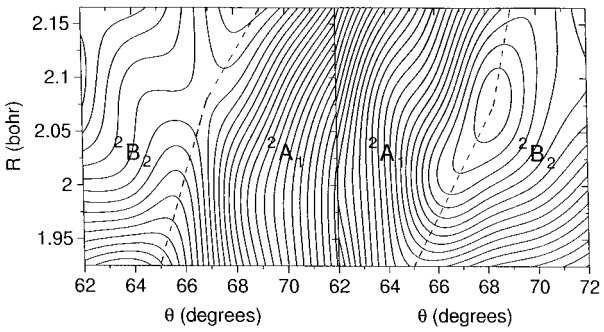

Figure 2. $\tilde{A}^2A_1/\tilde{B}^2B_2$ conical intersection. Contour plots of the $1^2A'$ (left) and $2^2A'$ (right) adiabatic potentials, with energy in hartree with respect to the $\tilde{X}^2B_1$ minimum and ΔE = 0.001 hartree. The dashed line shows the intersection locus. $1^2A'$ (left): innermost contours at 0.175 hartree; the energy is increasing or decreasing along or perpendicular to the intersection locus, respectively. $2^2A'$ (right): innermost minimum contour at 0.175 hartree.

$^2B_2$ or $^2A_1$ on the left or on the right of the intersection line, respectively, and vice versa for the upper $2^2A'$ state. The CI potentials have been calculated at 48 points (R,θ) and have been interpolated with the spline technique. Owing to the limited number of points, the interpolation masks the discontinuity of the surfaces at the intersection locus, which is also slightly different in the two contour plots. Nevertheless, the $1^2A'$ saddle region or the $2^2A'$ minimum valley along the intersection and the greater slope of the $^2A_1$ regions are clearly recognizable. We estimate that the intersection minimum is at R = 2.08 ± 0.02 bohrs and θ = 67.5 ± 1°, with energy equal to 38 400 ± 100 cm^{-1} with respect to the $\tilde{X}^2B_1$ minimum, *i.e.* about 2100 cm^{-1} above the $\tilde{B}^2B_2$ T_e value. These results are close to the corrisponding ones for the H_2O^+ isoelectronic ion:[27] $R \approx 2.05$ bohrs and $\theta \approx 74.4°$, and $E \approx 38\,600$ cm^{-1}, *i.e.* about 2200 cm^{-1} above the $\tilde{B}^2B_2$ potential minimum.

According to the PB,[4] SLL,[9] and VZKDP[5] calculations, the 2^2B_1 is unbound, has a large $2^2B_1 \leftarrow \tilde{X}^2B_1$ transition moment, and should thus be very important in the NH_2 adiabatic photodissociation to NH($\tilde{a}^1\Delta$) + H. Nevertheless, the 2^2B_1 state correlates[4] with $1^2\Sigma^-$, which intersects[12] the $1^2\Pi$ species at $C_{\infty v}$, and therefore the 2^2B_1 can photodissociate nonadiabatically to NH($\tilde{X}^3\Sigma^-$) + H.

Figure 3 reports the $C_{\infty v}$ adiabatic potentials for the $1^2\Pi/1^2\Sigma^-$ conical intersection, which corresponds to a $1\pi/4\sigma$ MO crossing. The C_s symmetry of both states is $^2A''$, and the $C_{\infty v}$ symmetries are shown on the two sides of the intersection line. The minimum intersection point is at R_1 = 1.94 ± 0.02 bohr, R_2 = 3.12 ± 0.02 bohrs, and E = 41 200 ± 100 cm^{-1}, *i.e.* about 29 200 and 7400 cm^{-1} above the $NH_2(1^2\Pi)$ and NH($\tilde{X}^3\Sigma^-$) + H equilibrium structures, to which converge the $^2\Pi$ or $^2\Sigma^-$ sheets of the $1^2A''$ surface, respectively. Note that this lowest-energy point represents the barrier for the ground-state collinear reaction NH + N → NH_2, that this barrier is removed in C_s symmetry,[5] and that the $1^2\Sigma_g^-$ saddle point at $D_{\infty h}$ is at 47 967 cm^{-1} and R = 2.555 bohrs. The $1^2\Pi$ main configuration is changed from $3\sigma^21\pi^3$ to $3\sigma1\pi^34\sigma$, according to the configuration of the NH($\tilde{X}^3\Pi$) + H dissociation products. On the contrary, the $1^2\Sigma^-$ species keeps its $3\sigma^21\pi^24\sigma$ configuration, equal to that of NH($\tilde{X}^3\Sigma^-$) + H, but the character of the 4σ MO is now changed from Rydberg 3s of N to valence 1s of H.

5. Conclusions

The present MRD-CI calculations have been carried out with a large AO basis of 122 contracted Gaussian functions and by correlating seven electrons among 120 NOs of each electronic state. By including in the reference set all the configurations

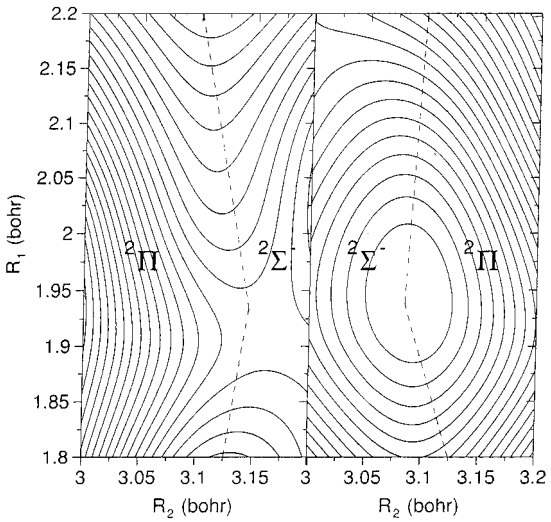

Figure 3. $1^2\Pi/1^2\Sigma^-$ conical intersection. Contour plots of the $1^2A''$-(left) and $2^2A''$(right) adiabatic potentials with energy in hartree with respect to the $\tilde{X}^2B_1$ minimum and $\Delta E = 0.001$ hartree. The dashed line shows the intersection locus. $1^2A''$ (left): innermost contours at 0.188 hartree; the energy is increasing or decreasing along or perpendicular to the intersection locus, respectively. $2^2A''$ (right): innermost minimum contour at 0.188 hartree.

with a weight of at least 0.001, the NO basis minimizes the dimensions of the reference and of the selected spaces and always gives a reference contribution larger than 0.96.

We have calculated the equilibrium structures, the adiabatic and vertical transition energies, the barriers to linearity, and the dissociation energies of the $\tilde{X}^2B_1$, $\tilde{A}^2A_1$, and $\tilde{B}^2B_2$ electronic states. The corresponding experimental values have been well reproduced, and previous calculations have been improved. The barriers to linearity of the first two species are in good agreement with the best results deduced from experiment, and the differences between the theoretical and the observed dissociation energies are smaller than 2.5%. The low-angle structure of $\tilde{B}^2B_2$ has been confirmed, and we have shown that this state has a very flat C_{2v} potential in the equilibrium region and that it is bound with respect to the NH + H and N + H_2 dissociation limits. We have finally investigated the potentials of the $\tilde{A}^2A_1/\tilde{B}^2B_2$ and $1^2\Pi/1^2\Sigma^-$ pairs, which intersect conically at energies greater than 38 000 cm^{-1}. The corresponding nonadiabatic effects should thus not affect the rovibronic spectrum of the $\tilde{X}^2B_1$ and $\tilde{A}^2A_1$states, but they should be more important for the NH_2 photodissociations.

Acknowledgment. The authors are very grateful to Professor R. J. Buenker for a copy of the MRD-CI programs. This work has been supported by the Consiglio Nazionale delle Ricerche (Grant 95.01187.CT03 and Istituto di Chimica Quantistica ed Energetica Molecolare di Pisa) and by the Ministero dell'Università e della Ricerca Scientifica e Tecnologica (grants 40% and 60%).

References and Notes

(1) Herzberg, G.; Ramsay, D. A. *J. Chem. Phys.* **1952**, *20*, 347.
(2) Dressler, K.; Ramsay, D. A. *Philos. Trans. R. Soc. London A* **1959**, *251*, 553.
(3) Bell, S.; Schaefer, H. F., III. *J. Chem. Phys.* **1977**, *67*, 5173.
(4) Peyerimhoff, S. D.; Buenker, R. J. *Can. J. Chem.* **1977**, *57*, 3182.
(5) Vetter, R.; Zülicke, L.; Koch, A.; van Dishoeck, E. F.; Peyerimhoff, S. D. *J. Chem. Phys.* **1996**, *104*, 5558.
(6) Jungen, C.; Hallin, K. J.; Merer, A. J. *Mol. Phys.* **1980**, *40*, 25.
(7) Buenker, R. J.; Peric, M.; Peyerimhoff, S. D.; Marian, R. *Mol. Phys.* **1981**, *43*, 987.
(8) Gabriel, W.; Chambaud, G.; Rosmus, P.; Carter, S.; Handy, N. C. *Mol. Phys.* **1994**, *81*, 1445, and references therein.
(9) Saxon, R. P.; Lengsfield, B. H., III; Liu, B. *J. Chem. Phys.* **1983**, *78*, 312.
(10) Biehl, H.; Schönnenbeck, G.; Stuhl, F.; Staemmler, V. *J. Chem. Phys.* **1994**, *101*, 3819, and references therein.
(11) Petrongolo, C.; Hirsch, G.; Buenker, R. J. *Mol. Phys.* **1990**, *70*, 825.
(12) Carter, S.; Mills, I. M.; Dixon, R. N. *J. Mol. Spectrosc.* **1984**, *106*, 411.
(13) Buenker, R. J.; Peyerimhoff, S. D. *Theor. Chim. Acta* **1974**, *35*, 33.
(14) Knowles, D. B.; Alvarez Collado, J. R.; Hirsch, G.; Buenker, R. J. *J. Chem. Phys.* **1990**, *92*, 585, and references therein.
(15) Huzinaga, S.; Klobukowski, M.; Tatewaki, H. *Can. J. Chem.* **1985**, *63*, 1812.
(16) van Duijneveldt, F. B. *IBM Res. Rep.* **1971**, RJ945.
(17) Raffenetti, R. C. *J. Chem. Phys.* **1973**, *58*, 4452.
(18) Dunning, T. H., Jr. *J. Chem. Phys.* **1989**, *90*, 1007.
(19) Dunning, T. H., Jr.; Hay, P. J. In *Modern Theoretical Chemistry*; Schaefer, H. F., III, Ed.; Plenum: New York, 1977; Vol. 2, Chapter 1.
(20) Wright, J. S.; Barclay, V. J.; Buenker, R. J. *Chem. Phys.* **1987**, *115*, 23, and references therein.
(21) Herzberg, G. *Molecular Spectra and Molecular Structure*; Van Nostrand Reinhold: New York, 1966; Vol. 3, p 584.
(22) Halpern, J. B.; Hancock, G.; Lenzi, M.; Welge, K. H. *J. Chem. Phys.* **1975**, *63*, 4808.
(23) Gibson, S. T.; Greene, J. P.; Berkovitz, J. *J. Chem. Phys.* **1985**, *83*, 4319.
(24) Huber, K. P.; Herzberg, G. *Molecular Spectra and Molecular Structure*; Van Nostrand Reinhold: New York, 1979; Vol. 4.
(25) Moore, C. H. *Atomic Energy Levels*; Nat. Bur. Stand.: Washington, DC, 1949; Vol. I.
(26) Staemmler, V.; Jaquet, R. *Theor. Chim. Acta* **1981**, *59*, 501.
(27) Jackels, C. F. *J. Chem. Phys.* **1980**, *72*, 4873.